Responsivity Calibration of the QUIET Q-band Array

Robert N. Dumoulin✠ for the QUIET collaboration

Columbia University, 550 W 120th Street, New York, NY, 10027, USA.

ABSTRACT

The Q/U Imaging ExperimenT (QUIET), a ground-based experiment located in the Atacama Desert in Chile, measures the polarization of the Cosmic Microwave Background (CMB). In Phase I, it measures the CMB polarization at angular scales of $25 \lesssim l \lesssim 1000$ using radiometer arrays in the Q (44 GHz) and W (95 GHz) frequency bands. The Q-band and W-band receivers of Phase I of the QUIET instrument contain 2 and 6 total power modules (TT modules), and 17 and 84 polarization modules respectively. Responsivities for the TT modules are obtained primarily from Jupiter and skydip measurements, using Jupiter as the absolute calibrator and the more frequent skydip measurements to track short time-scale fluctuations over the course of the season. Responsivities for the polarization modules are obtained from Tau A, relative measurements from the Moon, a polarizing wire-grid, and skydips. Skydips are used to track the responsivity of the polarization modules on a shorter time-scale.

Keywords: QUIET, cosmic background radiation, cosmology observations, telescopes, instrumentation: polarimeters, methods: data analysis

1. INTRODUCTION

The Q/U Imaging ExperimenT (QUIET) is a ground-based experiment that collects cosmic microwave background (CMB) data. In Phase I, it measures CMB polarization in the Q (44 GHz) and W (95 GHz) frequency bands.[1,2] Polarization anisotropy in the CMB contains a wealth of information. It can be decomposed into two components: E-modes and B-modes. E-modes can tighten constraints on cosmological parameters; the detection of primordial gravity wave B-modes could lead to the confirmation of inflationary theory or to ruling out large classes of inflationary models. For Phase I, QUIET's primary goals are to characterize E-modes at angular scales of $25 \lesssim l \lesssim 1000$. QUIET Phase II will map the CMB polarization angular power spectrum up to angular scales of $l \sim 2000$ and constrain the tensor-to-scalar ratio to $r \simeq 0.01$.

The QUIET Phase I instrument (hereafter "QUIET" will refer to QUIET Phase I) consists of two independent polarimeter arrays which observe the sky from the former CBI[3] site (hereafter QUIET site), located in the Chajnantor plateau of the Atacama desert in Chile. The Q-band array was placed on the former CBI mount and observed between October 2008 to June 2009. After completing Q-band observations, the W-band array was then deployed and W-band observations have been ongoing since August of 2009. Here we discuss the responsivity calibration of the Q-band receiver.

For Phase I, the QUIET Q-band array consists of 17 polarization modules and 2 total power modules (hereafter TT modules). The QUIET polarization modules are capable of measuring both intensity (proportional to the CMB temperature) and polarization. Light enters a cryogenically cooled platelet array of corrugated feedhorns[4] and is split into left- and right- circularly polarized components by a septum polarizer orthomode transducer (OMT).[5] Each polarized component enters independent legs of the QUIET module,[6] and each leg is amplified and phase switched (one leg at 4kHz, the other at 50Hz), and coupled by a 180 degree hybrid coupler. The output of the coupler is separated into two: half of the signal rectified and detected by a set of detector diodes, and the other half coupled by a 90 degree hybrid coupler and detected by a second set of detector diodes. There are four readout channels per QUIET module, Q1, Q2, U1, U2, nominally measuring $+Q$, $-Q$, $+U$, $-U$ respectively. Summing the output of an individual detector diode, first at 4kHz and then at 50 Hz, yields a measurement of the intensity (I), which we refer to as the averaged time stream. Differencing instead of summing yields a measurement of the Stokes $\pm$Q parameters on the first set of detector diodes, and the Stokes $\pm$U parameters

✠ robert@phys.columbia.edu

on the second set of detector diodes. The differenced outputs are referred to as the double demodulated time stream (hereafter demodulated time stream). The averaged time stream suffers from large $\frac{1}{f}$ noise (which the demodulated time stream does not suffer from) and is therefore not used for science measurements, though it is still important for calibration. The Q-band TT modules are adjacent to one another in the array, and the outputs from their X-Y OMTs are routed via magic tees, such that we measure the differential signal between the two TT modules.[7] A more in depth look at how the total power and demodulated time streams are obtained from the QUIET modules can be found in these proceedings.[8]

QUIET observes CMB patches using a constant-elevation scan (CES), by scanning back and forth in azimuth at a constant elevation while the patch moves through the scan region by sidereal motion. Calibrations sources are generally observed using a raster scan, which involves elevations steps as well as azimuth scans. Our calibration sources provide us with crucial information regarding the function and performance of the QUIET receiver, such as the responsivity of our detector diodes, the detector angle (with respect to Stokes parameters Q and U) of each module, the observed leakage from total power to Q and U polarizations ($I \rightarrow Q/U$), and the white noise of each detector diode. For the sake of brevity for this proceeding, this article will only examine the responsivity calibration of both the TT and polarization modules. The responsivity of a diode [mV/K] is the change of the measured signal on the Q and U diodes [mV] to that of the observed polarization [K]. We divide our calibration sources into two classifications: absolute and relative. Absolute calibrators are those used to determine the absolute scale of our responsivities. Relative calibrators are those used to relate the responsivity of a given diode to that of a reference diode (which we have chosen to be the +Q diode on the central module).

After we define an equation for the responsivity of our detector diodes in §2, we then examine our calibration sources for the TT and polarization modules and explain how we extract responsivities from them in §3 and §4. We then outline our two gain models for calculating the responsivity of each diode in §5, and the sources of errors involved with the two models in §6.

2. CHARACTERIZING THE RESPONSIVITY OF QUIET DETECTOR DIODES

The variation in the responsivity with time of our QUIET detector diodes can be modeled primarily in terms of the temperature of the electronics enclosure, T_{enc}, which houses the electronics boards that bias the QUIET modules. Each detector diode, whether on a TT or polarization module, has both averaged and demodulated time-ordered data, and thus each diode has an averaged and demodulated responsivity. We individually characterize the responsivity of each detector diode using

$$R(T_{enc}) = R_o(1 + \beta(T_{enc} - T_o)), \tag{1}$$

where $R(T_{enc})$ is the responsivity of the detector diode, R_o is the magnitude of the responsivity at an enclosure temperature of T_o, β is the percentage change in responsivity per degree K change in enclosure temperature, and T_o is a reference point (universal to all detector diodes) for the temperature of the electronics enclosure. Typical values of R_o and β range from $1 < R_o$ [mV/K] < 4, and $0 < \beta$ [%/K] < 4. During normal operation, the responsivity of our detector diodes can fluctuate by as much as ∼5-10% over the period of several hours, and we must take account for this effect.

Averaged and demodulated responsivities depend on the gains g_A and g_B of legs A and B of the QUIET module.[8] The averaged responsivity is proportional to a linear combination of g_A^2 and g_B^2 and the demodulated responsivity is proportional to the product $g_A g_B$. While the averaged and demodulated responsivities (at our reference temperature T_o) of a particular diode, R_o, will be different, as long as the temperature dependences of the leg gains are similar in magnitude, the demodulated and total power responsivities will have the same dependence on enclosure temperature, β. Although we have both demodulated and averaged responsivities, it is the demodulated responsivities that are used in order to analyse QUIET data for CMB polarization maps, QUIET's primary science goal.

3. CALIBRATION STRATEGY

A general outline of how the calibration strategy is given below. Table 1 summarizes the calibration sources: how frequently the source is observed, whether it is used as a calibrator for TT or polarization modules, and whether it is used for absolute or relative calibration.

3.1 TT module calibration

- Demodulated Jupiter, RCW38 and Venus responsivity measurements provide the absolute calibration for the TT modules. Jupiter is the brightest unpolarized source that QUIET observes and is used as the principal calibrator, with RCW38 and Venus being used as consistency cross-checks. Over the course of the season we obtained 28 demodulated Jupiter responsivity measurements, roughly one every seven days. We reference QUIET's Q-band Jupiter measurements to the seven-year WMAP result.[9] Since WMAP's Q-band frequency (~ 40.6 GHz) is different from QUIET's, we linearly interpolate the WMAP result (using WMAP's Q- and V-band data) to QUIET's Q-band frequency.

- In order to determine short-timescale fluctuations in the responsivity with respect to the temperature of the electronics enclosure, we also use the more frequent skydip responsivity measurements, using the averaged data stream. Skydip measurements consist of three slews in elevation ($\simeq 6$ degrees in amplitude, peak-to-peak, taking 30 seconds per slew), during which we measure the change in brightness temperature of the atmosphere between the two elevations. Skydips are performed approximately every 1.5 hours (before each CES), and number $\sim$3000 over the Q-band season.

- In order to directly compare demodulated Jupiter/RCW38/Venus with averaged skydip responsitivities, a averaged-to-demodulated scaling factor, obtained from our Moon measurements, is applied to the skydip responsivities. The Moon, the brightest source which QUIET observes, provides us with high signal-to-noise averaged and demodulated data streams, and is ideal to determine our averaged-to-demodulated scaling factor. Corrective factors, including Ruze scattering and opacity factors, are also applied to the skydip responsivities.

3.2 Polarization module calibration

- Taurus A (Tau A, the Crab Nebula) is the brightest absolute polarized source that QUIET observes, and demodulated responsivity measurements of this source provide the absolute calibration for the polarization modules. Tau A was observed approximately every second night using the central horn (which includes our reference diode). 54 demodulated central horn responsivity measurements were made throughout the season, and each off-center horn was observed at least once throughout the season. Tau A measurements are referenced to the seven-year WMAP result, by interpolating the WMAP result (using WMAP's K-, Ka-, Q-, V- and W-band data, and fitting the result as a function of frequency) to QUIET's Q-band frequency.

- Weekly Moon raster scans and a single end-of-the-season polarizing wire-grid measurement (a wire-grid is rotated several times in front of the cryostat, allowing us to construct a well-defined polarized signal which is simultaneously observed by all of the modules) provide us with relative demodulated responsivities for each polarization diode with respect to the reference diode of our array.

- The absolute calibration of the central module is accomplished solely using Tau A measurements; absolute calibration of non-central modules is accomplished using their individual Tau A measurements, and the relative Moon and wire-grid measurements referenced to the mean value of the reference diodes' absolute Tau A measurements.

- Skydip measurements are used to determine short time-scale fluctuations (for each CES, every $\sim$1.5 of hours) in the responsivity as a function of the temperature of the electronics enclosure temperature (see §2) for the polarization modules.

Source	Frequency of observation	TT/polarization	absolute/relative
Jupiter	weekly	TT	absolute
RCW38	weekly	TT	absolute
Venus	every second week	TT	absolute
Tau A	every 1-2 days	polarization	absolute
Moon	weekly	TT/polarization	relative
wire-grid	once; end-of-season	polarization	relative
skydips	$\sim$ every 1.5 hours	TT/polarization	relative

Table 1. Summary of QUIET calibration sources

4. OBTAINING RESPONSIVITIES FROM OUR CALIBRATION SOURCES

We will now look at how we extract the responsivity of our detector diodes, $R(T_{enc})$, from each of our calibration sources. All equations in §4 are for an individual diode, and each TT and polarization diode is calibrated independently.

4.1 Absolute calibrators

4.1.1 Jupiter, RCW38 and Venus – Absolute demodulated responsivity (TT Modules)

Jupiter, RCW38, and Venus measurements provide the absolute calibration for the TT modules. Each source was observed using a raster over a time period of $15-30$ minutes. We model Jupiter/RCW38/Venus as point sources, and the demodulated responsivity of a source S, R_S, and $I \rightarrow Q/U$ leakage is obtained by binning the demodulated time-ordered data from the observation to create a map, and by fitting separate two-dimensional Gaussian fits to the positive and negative peaks of the map.

For Q-band, the interpolated antenna temperature of RCW38 is $\sim$40 mK (values vary slightly diode-to-diode depending on each diodes' central frequency and bandwidth), and the interpolated temperature of Jupiter and Venus, due to the varying distances of the planets from the Earth, are respectively $\sim$40-70 mK, and $\sim$40-300mK.

4.1.2 Tau A – Absolute demodulated responsivity (Polarization Modules)

Tau A provides the absolute calibration for the polarization modules. The demodulated responsivity of Tau A, R_T, is determined from the demodulated data stream. Tau A was observed with the central module approximately every other night, with one of the other modules being observed in between central module measurements (cycling through each element in the array). Each Tau A observation consists of six $\sim$6-minute raster scans, rotating the deck of the telescope by 45° in between each scan. Changing the deck angle allows us to simultaneously fit for the responsivity, leakage and detector angle of each diode.

We model TauA as a point source whose amplitude is described by a two-dimensional Gaussian. The polarization signal amplitude (A_{TOD}) is extracted using the maximum-likelihood fit for demodulated time-ordered data for each deck observation, assuming a two-dimensional Gaussian beam shape. From this fit, we extract the amplitude, A, of the signal from Tau A, and define the absolute demodulated responsivity from each Tau A measurement, R_T, using

$$R_T = \frac{A}{T^{pol}_{TauA}}, \tag{2}$$

where T^{pol}_{TauA} is the temperature of the polarized flux density of Tau A. The temperature of the polarization flux density of Tau A, interpolated from WMAP data, is $\sim$5 mK for QUIET's Q-band frequency (values vary slightly diode-to-diode depending on each diodes' central frequency and bandwidth). A map of Tau A, constructed from observations of the +Q diode of the central module, is seen in Figure 1 (a). The map is normalized to its maximum value.

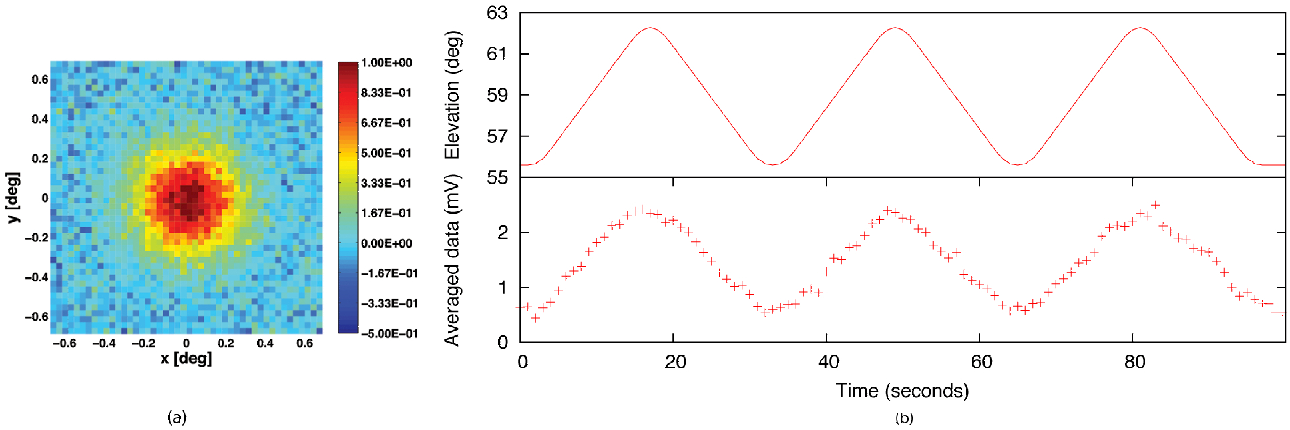

Figure 1. (a) Normalized Tau A map using the +Q diode of the central module in instrumental coordinates. (b) The elevation and total power data stream (total power data stream is adjusted by a constant offset) is shown for a typical skydip. As the elevation of the telescope is oscillated, the amplitude of the total power signal oscillates as well.

4.2 Relative calibrators

4.2.1 Moon – Relative demodulated responsivity (TT & Polarization Modules)

We obtain demodulated responsivities of each polarization detector diode, R_M^{rel} (relative to our reference diode), using observations of the Moon. The amplitude of the signal from the Moon is large relative to other calibration sources, making it a desirable relative calibration source (compare the Q-band peak polarization temperature of the Moon (∼2 K) to that of Tau A (∼5 mK)) and QUIET is able to detect the Moon's polarized emission with a signal-to-noise ratio of greater than 1000 in one second of observing.

We use a simple physical model for the Moon, assuming it to be a dielectric sphere at a uniform temperature, and determine the amplitude of the demodulated responsivity, R_M, by fitting the demodulated data stream $\mathcal{F}$ using

$$\mathcal{F} = R_M[Q\cos(2\chi) + U\sin(2\chi)] + \mathcal{F}_0 + \eta, \tag{3}$$

where $\mathcal{F}_0$ is a fitted offset parameter, Q and U are the polarized Stoke's parameter signals from the Moon, χ is the detector angle of the module defined to a specified reference angle, and η represents the amount of $I \rightarrow Q/U$ leakage into the demodulated stream.

To calibrate the absolute responsivity using moon measurements, one must characterize effects related to:

1. Change in temperature of the Moon with its lunar phase.
2. Change in Q and U polarizations over the face of the Moon.
3. The angular diameter of the the moon (∼28 arcmin). Care must be taken as the Q-band beam size is ∼27 arcmin.

We therefore use the moon measurements as a relative rather than absolute calibrator, normalizing the fit value of each polarization diode, R_M, to the reference diode to obtain R_M^{rel}

The Moon is also used in order to get our averaged-to-demodulated scaling factor for the TT diodes. These factors are obtained by averaging the ratio of the average data stream to that of the demodulated data stream over the duration of the Moon measurement for each TT diode.

4.2.2 Wire-grid – Relative demodulated responsivity (Polarization Modules)

QUIET uses a polarising wire-grid to determine the demodulated responsivity of a polarization diode relative to the reference diode, R_W^{rel}. QUIET's polarizing wire-grid consists of an array of fine metallic wires parallel to one another in a plane. The measurement is performed at the end of the season by rotating the wire-grid directly in front of the cryostat window, with the plane of the wire-grid parallel to the plane of the cryostat window. As the wire-grid is rotated in front of the cryostat, the component of the electric field that is aligned parallel to the wires induces electron movement along the wires, and this component is reflected back in the direction of incidence. We obtain the demodulated responsivity of a polarization diode, R_W, by fitting the demodulated data stream $\mathcal{F}$ using

$$\mathcal{F} = R_W W_0 \sin(2(\omega t - \chi)) + \mathcal{F}_0, \tag{4}$$

where $\mathcal{F}_0$ and χ are respectively the fitted offset parameter and phase angle, W_0 is the polarization power from the wire-grid, ω is the angular frequency at which the wire-grid is being rotated (2ω is the angular frequency of the polarization rotation, as the wire-grid is 180° symmetric), and t is the time. We normalise the fit value of R_W for each diode to our reference diode to obtain R_W^{rel}.

4.2.3 Skydips (TT & Polarization Modules)

Skydips are performed before each CES in order to determine a frequent measure of the change in responsivity with time, R_s. Figure 1 (b) shows the telescope elevation and averaged data stream as a function of time for a typical skydip.

The responsivity from the averaged data stream, R_s, is obtained for each skydip measurement by fitting the averaged data stream $\mathcal{F}$ using

$$\mathcal{F} = R_s T_B + \mathcal{F}_0, \tag{5}$$

where $\mathcal{F}_0$ is a fitted offset parameter, and T_B is the brightness temperature of the atmosphere described as

$$T_B = T_{atm}(1 - e^{-\frac{\tau_0}{\sin(\theta)}}), \tag{6}$$

where T_{atm} is physical temperature of the atmosphere, θ is the elevation angle of the telescope, and τ_0 is the zenith opacity of the atmosphere at the site (which is a function of precipitable water vapour (PWV) and ground temperature (T_{ground}), $\tau_0 = f(\mathrm{PWV}, T_{ground})$).

For each skydip, we fit for the product of the averaged data stream responsivity and the atmospheric temperature, which we denote by Δ,

$$\Delta = R_s T_B, \tag{7}$$

and use this as an input into our gain models.

5. CALCULATING TT AND POLARIZATION RESPONSIVITIES

5.1 QUIET Data Analysis Pipelines

The QUIET data analysis effort consists of two independent analysis pipelines, one using a maximum likelihood (hereafter ML) tools for map-making and power spectrum estimation,[10] and the other using a Pseudo-C_ℓ (hereafter PCL) analysis that employs a Pure E- and B-mode estimator.[11] The responsivities of the ML and PCL pipelines are calculated using independently constructed gain models. Both gain models account for local weather conditions at the Chajnantor site and describe the short time-scale variability in the responsivity of each diode as a function of the temperature of the electronics enclosure (equation (1)), which is sampled at 1 Hz.

While the ML and PCL gain models use the same calibrators and share the same general formula for the responsivity, the method via which they acquire values of R_o and β and the way in which they are implemented in the analysis is different. Here we examine how the ML gain model obtains demodulated responsivities, and briefly describe the differences between the ML and PCL gain models.

5.2 ML gain model

This section demonstrates how the ML gain model obtains demodulated responsivities for the TT and polarization modules, and how it is implemented into the pipeline. The ML gain model determines a single value of R_o and β over the entire season for each diode, such that the demodulated responsivity of any diode is a function of the temperature of the electronics enclosure, and can be calculated as frequently as every sample.

5.2.1 Model of TT gains

As seen from §4.2.3, skydip measurements are the product of the averaged data stream responsivity and the brightness temperature of the atmosphere at the site (equation 7), which depend not only on the enclosure temperature, but also on the PWV and ground temperature, T_{ground}, at the site. We seek to separate these values into a responsivity for each diode which varies only with enclosure temperature, and a brightness temperature of the atmosphere which depends on PWV and T_{ground}. Two atmospheric models, AM[12] and ATM,[13] give the brightness temperature of the Chajnantor sky as a function of PWV and T_{ground}. For our frequency range of interest, the AM and ATM models predict different zenith brightness temperatures of the atmosphere for a given PWV and T_{ground}. The variation in brightness temperature between the two models though, as a function of PWV and T_{ground}, is within 4% of each other (in our frequency and PWV range of interest for the Q-band array). We use the ATM model to describe the variation in the brightness temperature of the atmosphere (changing from the ATM model to the AM model resulted with a difference of <1% in our determined values of R_o and β for each diode). The absolute scale of the brightness temperature, however, is set by the QUIET data. QUIET obtains PWV and T_{ground} measurements from the Atacama Pathfinder EXperiment (APEX) weather station every minute, located within 3 km of the QUIET site.

Skydip measurements are scaled by the following factors in order to compare the responsivities of demodulated and averaged time streams:

1. Each skydip responsivity is scaled by the mean ratio of the averaged-to-demodulated data from the Moon measurements.
2. Ruze scattering,[14] a loss effect due to the roughness of the telescope surface, scatters away source radiation. This correction factor does not change significantly over the bandpass of our Q-band modules, and the same factor is applied to each skydip responsivity.
3. Opacity correction. The opacity correction factor at the QUIET site is small (∼3%) and its variation for each detector diode is negligible compared to other uncertainties (<0.5%). Since the absolute calibration of the QUIET detector diodes come from astronomical source observations, the opacity is already taken into account in the absolute calibrations. A second-order correction factor, to account for the variation in opacity seen by each QUIET detector diode is applied to the skydip responsivities.

Skydip measurements that have been adjusted by the above scaling and correction factors (and can be now directly compared to demodulated gain values) will be denoted by Δ^*. Using the demodulated source measurements (see §4.1.1) in conjunction with the total power skydip measurements, we are able to break the degeneracy between R_s and T_B in the skydip measurements Δ^* by maximizing the joint likelihood of the source and skydip measurements. The likelihood of the i^{th} source measurement is calculated using

$$\mathcal{L}_i^S = \frac{1}{\sigma_i\sqrt{2\pi}} \exp[-\frac{(m_i - (R_o(1+\beta(T_{enc}-T_o))))^2}{2\sigma_i^2}], \tag{8}$$

where we fit for R_o and β, and $m_i \pm \sigma_i$ are the source responsivity measurements R_S with corresponding random error. Including all of the source measurements,

$$\mathcal{L}^S = \prod_{i=1} \mathcal{L}_i^S. \tag{9}$$

The likelihood of the skydip measurements is obtained using $\mathcal{L}_j^s$, which for the j^{th} skydip is

$$\mathcal{L}_j^s = \frac{1}{\sigma_j\sqrt{2\pi}} \exp[-\frac{(m_j - (R_o(1+\beta(T_{enc}-T_o))) \cdot T_B(PWV, T_{ground}))^2}{2\sigma_j^2}], \tag{10}$$

where we fit for R_o, β and $T_B(PWV, T_{ground})$, and $m_j \pm \sigma_j$ is the fitted value of Δ^* with corresponding random error. Including all of the skydip measurements,

$$\mathcal{L}^s = \prod_{j=1} \mathcal{L}_j^s, \tag{11}$$

and the joint likelihood of the source and skydip measurements is defined to be

$$\mathcal{L} = \mathcal{L}^S \mathcal{L}^s. \tag{12}$$

From simultaneously maximizing the likelihood of the source and skydip measurements we determine the absolute value of the responsivity R_o and the percentage change in responsivity as a function of enclosure temperature β for each TT diode. The obtained values of R_o and β can then be used to calculate the demodulated responsivity of our TT diodes for any time given the temperature of the enclosure using equation (1). The brightness temperature of the Chajnantor sky is also determined by the simultaneous likelihood fit process and can be compared to other measurements as a cross-check (the TT modules are designed to measure absolute temperature, and the value of the brightness temperature of the sky that they obtain is also used for the polarization modules).

5.2.2 Model of Polarization Gains

Once we have reduced our Tau A, Moon and wire-grid data, we are able to determine the amplitude of the demodulated responsivity for each polarization module diode at our reference temperature T_o. The value of R_o for the central module, with its 54 polarized Tau A measurements, is determined entirely by Tau A observations using

$$R_o = (\sum_{i=1}^{N_T} w^i R_T^i)/(N_T), \tag{13}$$

where R_T^i is the i^{th} (of N_T) Tau A central module demodulated responsivity measurement of the season, and w^i is the weight of the i^{th} Tau A measurement, given by

$$w^i = ((\sigma^i)^2)/(\sum_i (\sigma^i)^2). \tag{14}$$

For modules other than the central module, we use a combination of the small number of individual Tau A observations, along with relative Moon and wire-grid measurements to express the magnitude of the demodulated responsivity at our reference temperature T_o, given by

$$R_o = (\sum_{i=1}^{N_T} w^i R_T^i + \sum_{j=1}^{N_M} w^j R_M^{rel\ j} R_o^{ref} + w^w R_W^{rel}\ R_o^{ref})/(N_T + N_M + N_W), \tag{15}$$

where R_T^i is the i^{th} (of N_T) off-center module Tau A demodulated responsivity measurement, $R_M^{rel\ j}$ is the j^{th} (of N_M) relative demodulated Moon responsivity measurement of the season, R_W^{rel} is the single ($N_W = 1$) relative demodulated wire-grid measurement, and R_o^{ref} is the mean weighted value of the demodulated responsvitiy of the reference diode of the central module (from equation (13)).

Recalling from §2 that the variation in responsivity as a function of enclosure temperature is the same for the averaged and demodulated time-streams, we use the averaged time-stream of the polarization modules to determine our value of β. Given that the TT and polarization modules see the same brightness temperature of

the sky, we use the value of $T_B(PWV, T_{ground})$ obtained from the TT modules, and maximize the likelihood of equation (11) to obtain β. Using our above values for R_o (given by equations (13) and (15)) and β we construct a responsivity formula for each polarization diode using equation (1).

5.2.3 Implementation of ML Gain Model

Using the above process, we obtain values for the absolute demodulated responsivity, R_o, and the variation with respect to enclsoure temperature, β, for the TT and polarization modules. The ML pipeline uses these parameters in order to calculate the demodulated responsivity of each diode on timescales of 30 seconds, using the closest temporal enclosure temperature measurement (though the responsivity can be calculated as often as every second).

5.2.4 Example of ML gain model

An example of the demodulated responsivity for a single TT diode over the course of the Q-band season (for the +Q diode of module 17) calculated using the ML gain model, can be seen in Figure 2 (a). The value of the demodulated responsivity steadily decreases, resulting from an ∼1K drift in the enclosure temperature over the Q-band season. The ML gain model can calculate the demodulated responsivity every second, and an example of a demodulated time-ordered data stream divided by:

1. the average demodulated responsivity of the scan;
2. the ML gain model responsivity;

can be seen in Figure 2 (b). Ideally, if there is no variation in enclosure temperature, our demodulated signal should be a constant for each CES, with the only variation in the signal coming from white noise.

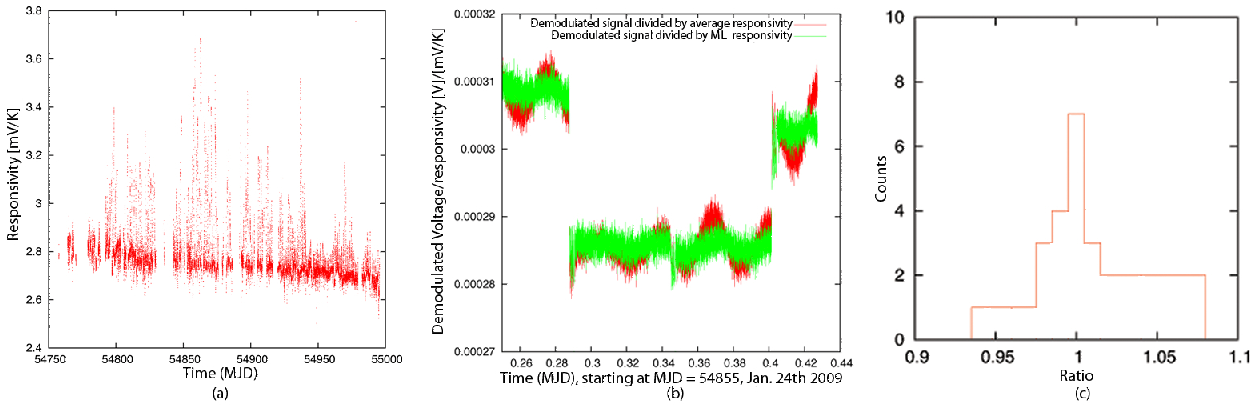

Figure 2. (a) Demodulated responsivity for a TT diode using the ML gain model over the course of the season. Larger spikes in the responsivity correspond to brief periods of time where the electronics enclosure lost regulation. (b) Demodulated time-ordered data for one diode for four CES scans, divided by 1) the mean demodulated responsivity of each CES, and 2) demodulated responsivity from the ML gain model. The demodulated data stream shown in (b) is an example of a time-period where we experienced significant enclosure temperature variation (∼2 K), and is not typical of most of our QUIET data (normally < 1 K variation throughout a CES), and was chosen to show the ability of the model to correct our data. The model is not able to remove all of the enclosure temperature dependence as there is a small amount of hysteresis, however uncorrected variations create errors one the order of $\sim 1 - 2\%$. (c) Ratio of measured Jupiter to calculated model demodulated responsivities.

Figure 2 (c) shows a histogram of the ratio of the measured Jupiter to calculated gain model demodulated responsivities over the course of the season (for the +Q diode of module 17). The histogram of measured Jupiter to calculated model demodulated responsivities is centered at 1.01 with a standard deviation of 0.03, which shows that the measured Jupiter responsivities are consistent with the calculated model responsivities.

5.2.5 Differences between the ML and PCL gain models

The PCL gain model is independently calculated in a manner similar to the ML gain model, but there are a couple of notable differences:

1. Instead of using an atmospheric model, the PCL gain model empirically fits the change in atmospheric temperature as a function of PWV, in order to take out atmospheric effects in the skydip measurements.
2. The PCL gain model calculates demodulated responsivities for TT and polarization diodes at the beginning of each CES (hence, every couple of hours).

6. SOURCES OF ERROR

The statistical and systematic errors for the ML and PCL gain model are calculated in a similar manner.

6.1 Statistical errors

The ML gain model calculates the statistical error of the responsivity of a diode using standard quadrature error formulae, and is described by

$$\sigma^2_{R(T_{enc})} = (1+\beta(T_{enc}-T_o))^2\sigma^2_{R_o} + R^2_o(T_{enc}-T_o)^2\sigma^2_\beta + R^2_o\beta^2\sigma^2_{T_{enc}}, \tag{16}$$

where σ_{R_o}, σ_β, and $\sigma_{T_{enc}}$, are the random errors of R_o, β, and T_{enc}. We are currently investigating correlations between errors.

6.2 Systematic errors

Although the methods for absolute calibration of the TT and polarization modules are different, both types of modules share the following systematics: systematic error incurred from our absolute calibrators; use of a model to determine the atmospheric temperature (comparing the results obtained from using the AM, ATM, and linear empirical fits to describe the variation in atmospheric temperature); uncertainty in the calculated beam size from map integration[7] with that of a Hermite-Guassian fit;[15] uncertainty in the shape and position of the bandpass (shifting the bandpass from its central frequency, or broadening or narrowing the bandpass); uncertainty in enclosure temperature (enclosure temperature hysteresis and systematic shift effect); and an uncertainty in the PWV at the site (given that the APEX weather monitor is located near but not at the QUIET site). Since the responsivities of the polarization diodes are relative to the reference diode in the array, the effect of changing the reference diode to any other diode in the array is also examined.

At the time of writing, the estimate of each of the above systematic errors is preliminary and is therefore not presented. However, considerable work has been performed to identify their values: current knowledge indicates that all of the systematic errors are small enough to provide data of the accuracy required to meet QUIET's science goals.

7. CONCLUSIONS

This proceedings has addressed the calibration procedure of the demodulated responsivities for the QUIET Q-band array. The W-band receiver, still undergoing observations, will be calibrated in a similar manner to the Q-band receiver.

8. ACKNOWLEDGEMENTS

Support for the QUIET instrument and operations comes through the NSF cooper- ative agreement AST-0506648. Support also provided by AST-04-49809, DE-AC02- 05CH11231, JSPS KAKENHI (A) 20244041, NSF PHY-0355328, and by the Strategic Alliance for the Implementation of New Technologies (SAINT). Some work presented was performed on the Joint Fermilab - KICP Supercomputing Cluster, supported by grants from Fermilab, Kavli Institute for Cosmological Physics, and the University of Chicago. We are particularly indebted to the engineers who maintained and operated the telescope: J. Cortes, C. Jara, F. Munoz, and C. Verdugo.

REFERENCES

[1] Buder, I., "Q/U Imaging ExperimenT (QUIET): a ground-based probe of cosmic microwave background polarization," *Proc. SPIE* **7741** (2010).

[2] Newburgh, L., "Measuring CMB Polarization with QUIET: The Q/U Imaging ExperimenT," *Twelfth Marcel Grossmann Meeting on General Relativity* (2009).

[3] Padin, S. and others, "The Cosmic Background Imager," *PASP* **114**, 83–97 (Jan. 2002).

[4] Gundersen, J. and Wollack, E., "Millimeter Wave Corrugated Platelet Feeds," *Proceedings of the Technology Development for a CMB Probe of Inflation, Journal of Physics: Conference Series* **155** (2009).

[5] Bornemann, J. and Labay, V., "Ridge Waveguide Polarizer with Finite and Stepped-Thickness Septum," *IEEE Transactions on Microwave Theory and Techniques* **43** (1995).

[6] Kangaslahti, P. and others, "Planar Polarimetry Receivers for Large Imaging Arrays at Q-band," *IEEE MTT-S International* (2006).

[7] Monsalve, R., "Beam characterization for the QUIET Q-Band instrument using polarized and unpolarized astronomical sources," *Proc. SPIE* **7741** (2010).

[8] Cleary, K. A., "Coherent polarimeter modules for the QUIET experiment," *Proc. SPIE* **7741** (2010).

[9] Weiland, J. L. and others, "Seven-Year Wilkinson Microwave Anisotropy Probe (WMAP) Observations: Planets and Celestial Calibration Sources," (Jan. 2010).

[10] Eriksen, H. K. and others, "Joint Bayesian Component Separation and CMB Power Spectrum Estimation," *ApJ* **676**, 10–32 (Mar. 2008).

[11] Smith, K. M. and Zaldarriaga, M., "General solution to the E-B mixing problem," *Phys. Rev. D* **76** (Aug. 2007).

[12] Paine, S., "The am Atmospheric Model SMA Technical Memo 152, Revision 3," (2004). http://www.cfa.harvard.edu/sma/memos/152-03.pdf.

[13] Garand, L. and others, "Radiance and Jacobian intercomparison of radiative transfer models applied to HIRS and AMSU channels," *J. of Geophysical Research* **106**(D20), 24,017–24,031 (2001).

[14] Ruze, J., "The effect of aperture errors on the antenna radiation pattern," *Nuovo Cimento* **9** (1953).

[15] Pampaloni, F. and Enderlein, J., "Gaussian, Hermite-Gaussian, and Laguerre-Gaussian beams: A primer," (Oct. 2004).